Biochimica et Biophysica Acta 1854 (2015) 321–326

Contents lists available at ScienceDirect

Biochimica et Biophysica Acta

journal homepage: www.elsevier.com/locate/bbapap

Resolution of sub-nanosecond motions in botulinum neurotoxin endopeptidase: An evidence of internal flexibility☆

Raj Kumar [a], Shuowei Cai [b], Emmanuel Ojadi [b], Bal. R. Singh [a,*]

[a] Botulinum Research Center, Institute of Advanced Sciences, Dartmouth, MA 02747, USA
[b] Department of Chemistry and Biochemistry, University of Massachusetts, Dartmouth, MA 02747, USA

ARTICLE INFO

Article history:
Received 10 October 2014
Received in revised form 2 December 2014
Accepted 5 December 2014
Available online 9 January 2015

Keywords:
Fluorescence anisotropy decay
Molten globule
Protein flexibility
Botulinum toxin
Circular dichroism
Protein denaturation

ABSTRACT

Botulinum neurotoxins (BoNTs) are the most poisonous substances known to mankind, which act on the peripheral nervous system leading to flaccid paralysis. Although co-crystal structure of BoNT/A light chain (LC) reveals some unique features of the biological function of this molecule, structural characteristics in solution reveal its dynamic features, not available through the published crystal structures. In this study, we have examined internal flexibility of this molecule by measuring rotational correlation time as a function of viscosity, using frequency domain fluorescence anisotropy decay technique. Fluorescence anisotropy decay of BoNT/A LC resolved sub-nanosecond local motion (faster component), interpreted as internal flexibility of the molecule was affected significantly with viscosity. Both local and global movements were affected by viscosity, which indicates the accessibility of protein core and flexibility of overall structure. In conclusion, this work demonstrates the presence of flexibility in the internal peptide segments, which appears to play a significant role in BoNT/A LC biological function.

1. Introduction

Botulinum neurotoxins (BoNTs) are metalloproteinases which act on peripheral nerves and cleave one of the crucial components of neuroexocytosis, causing inhibition of acetylcholine release at nerve–muscle junctions. Toxin molecules have evolved with unique characteristics of high stability, specificity, and selectivity. These molecules are currently used to treat several neuromuscular disorders, such as strabismus, blepharospasm, hemifacial spasm and cervical dystonia, because of their biological activity at very low concentration exclusively at neuro-muscular junctions [1,2]. Because of extreme toxicity, BoNTs are also considered Class A biothreat agents. While all confirmed serotypes of BoNT (A–G) are highly toxic, and can be used both as biothreat and therapeutic agents, botulinum neurotoxin A (BoNT/A) is the most toxic, and has been most successfully used for the treatment of many disorders, and also for cosmetic purposes [3]. Structure–function relationship of BoNTs plays a critical role in developing further therapeutic applications and also in devising antidotes against botulism.

Each of the BoNTs has a unique trimodular structure consisting of a 50 kDa binding domain (H_{CC}), a 50 kDa translocation domain (H_{CN}), and a 50 kDa catalytic domain (LC). Since this protein has evolved with amazing specificity, and very unusual mechanism of substrate recognition involving active site and exosites, it is likely to possess substantial flexibility in its structure to accommodate a large surface interaction with the substrate. The solution structure of BoNT/A is flexible and different from the crystal structure [4–8]. Silvaggi et al. [9] have in fact observed limited flexibility of the active site, although those changes would not necessarily explain differential interaction of BoNT endopeptidases with their respective substrates. Published crystal structures explain some of these phenomena [10–13], including the role of two exosites, α and β. However, there is a lack of consistent structural information of the biologically active enzyme, which appears to exist as a molten globule [5,14]. For example, the crystal structure does not explain satisfactorily the role of SNARE motifs of SNAP-25, which was established earlier by Washbourne et al. [8].

Structural characteristics in solution reveal a major role of the dynamic structure in the functioning of a protein molecule which is important for the design of effective inhibitors. It has been already observed that inhibitors identified for in vitro experiments failed to work under in vivo conditions and vice versa [15], the endopeptidase active site shows substantial flexibility [9], suggesting that structural dynamics may play a major role in the interaction of BoNT endopeptidase with the inhibitors. An understanding of molecular dynamics of the BoNT/A endopeptidase itself may reveal a variety of ways to inhibit its action and rescue poisoned nerve cells.

Abbreviations: BoNT, botulinum neurotoxin; BoNT/A LC, botulinum neurotoxin light chain (LCA); LED, light emitting diode; DTT, dithiothreitol; CD, circular dichroism; RCT, rotational correlation time

☆ This work was in part supported by a grant from the NIH (1U01A1078070-01) and the US Army Medical Research (W81XWH-08-P-0705 and W81XWH-14-C-0070).

* Corresponding author at: Institute of Advanced Sciences, 78-540, Faunce Corner Mall Road, Dartmouth, MA 02747, USA. Tel.: +1 508 992 2042; fax: +1 866 709 1689.
E-mail address: bsingh@inads.org (B.R. Singh).

http://dx.doi.org/10.1016/j.bbapap.2014.12.004
1570-9639/

To unravel the dynamic molecular features, we have examined the internal flexibility of BoNT/A LC. Structural changes in BoNT/A LC with viscosity have been monitored by circular dichroism, fluorescence anisotropy, and correlated with its endopeptidase activity. Fluorescence and circular dichroism showed significant conformational change in BoNT/A LC with the viscosity of the solution. Frequency domain fluorescence anisotropy decay analysis provided impressive resolution of rapid and complex decays of fluorescence anisotropy that allows discrimination between static and dynamic state of micro-environment of BoNT/A endopeptidase in solution. Results showed strong internal flexibility in BoNT/A LC molecule, which may be important for its substrate specificity and other biological functions.

2. Material and methods

2.1. Material

BoNT/A LC was purified according to the procedure described previously [6] with some modifications. All the samples were dialyzed in 10 mM sodium phosphate buffer, containing 150 mM NaCl and 1 mM DTT, pH 7.3, and purity was checked by SDS-PAGE. Coomassie blue staining showed essentially a single band for all the batches of LC used in this study. His-tag SNAG (a fusion protein consisting of SNAP-25, GFP, and HIS tag, batch no. SNAG-His6169SR, MW ~55 kDa) [16] was used as substrate for activity measurement.

2.2. CD spectroscopy

CD spectra were recorded at 25 °C on a Jasco J715 spectropolarimeter equipped with a Peltier type temperature control system (model PTC-348W). The concentrations of LC samples in the range of 20–300 μg/ml were used for far-UV CD measurements. Temperature-induced unfolding of the LC polypeptide was followed by monitoring the CD signal at 222. LC samples dissolved in a buffer (10 mM sodium phosphate buffer, pH = 7.3, containing 150 mM NaCl) alone or with buffer containing different concentrations (10–50%) of glycerol, were heated at a rate of 1 °C/min, and the ellipticity was recorded at 222 nm.

2.3. Fluorescence measurement

Thermal denaturation of tertiary structure was monitored by recording intrinsic Trp fluorescence. Fluorescence recording was carried out by ISS K2 fluorimeter (Urbana-Champaign, IL). Excitation and emission slit width was 8 nm. To minimize inner filter effect, the absorbance of BoNT/A LC at 295 nm was kept below 0.1. For following the thermal denaturation by fluorescence we plotted the ratio of fluorescence intensity at 351 nm and 324 nm as a function of temperature. Samples were heated from 25 to 90 °C at a rate of 1 °C/min.

2.4. Analysis of fluorescence anisotropy decay measurements

Frequency-domain fluorimetry has been demonstrated earlier for the measurement of complex and/or rapid decay of protein fluorescence anisotropy. In this experiment we wanted to distinguish local mobility of intrinsic Trp probe of the protein from the global rotation of the protein. Time-resolved anisotropies are obtained from the frequency (ω)-dependent phase angle difference between the perpendicular (φ) and parallel (φ_{II}) components of the modulated emission ($\Delta_\omega = \varphi - \varphi_{II}$) and from the ratio of the amplitudes of the modulated component of the emission ($\Lambda_\omega = m_{II}/m_\perp$). These values were fit through a multiexponential anisotropy decay law

$$r(t) = \sum r_i g_j e^{-t/\varphi i} \tag{A}$$

where φ_i is the correlation time, g_i is the associated amplitude, and r_i is the anisotropy of each component. The expected values of Δ_ω ($\Delta_{c\omega}$) and Λ_ω ($\Lambda_{c\omega}$) are calculated from the sine and cosine transforms of the individual polarized decays.

$$Ni = \int I_i(t)\ \sin\ \omega t\ dt \tag{B}$$

$$Di = \int I_i(t)\ \cos\ \omega t\ dt \tag{C}$$

The frequency-dependent values of Δ_ω and Λ_ω are given by

$$\Delta_{c\omega} = \arctan\{(D\,N - N\,D)/(N\,N + D\,D)\} \tag{D}$$

$$\Lambda_{c\omega} = \left\{\left(N^2 + D^2\right)/\left(N^2 + D^2\right)\right\} \tag{E}$$

where *Ni* and *Di* are calculated at each frequency. The parameters describing the anisotropy decay are obtained by minimizing the squared deviations between measured and calculated values,

$$\chi^2 = \sum (\Delta_\omega - \Delta_{c\omega})^2/\sigma^2{}_{\Delta\omega} + \sum\left((\Lambda_\omega - \Lambda_{c\omega})^2/\sigma^2{}_{\Lambda\omega}\right). \tag{F}$$

In this expression $\sigma_{\Delta\omega}$ and $\sigma_{\Lambda\omega}$ are the estimated experimental uncertainties in the measured quantities (Δ_ω and Λ_ω). The goodness-of-fit is usually judged by the value of reduced χ^2,

$$\chi_R{}^2 = \chi^2/\upsilon = \chi^2/2N\text{–}p$$

where υ, the number of degree of freedom, is given by $\upsilon = 2\,N - p$. N is the number of modulation frequencies and p is the number of floating parameters. If the assumed model is appropriate for the sample, and if the errors are random and properly estimated by $\sigma_{\Delta\omega}$ and $\sigma_{\Lambda\omega}$, then χ^2_R is expected to be near unity.

Eq. (A) can be expressed in another form:

$$r(\tau) = \frac{\alpha r_0}{1 + (1/\varphi_\tau + 1/\varphi_P)\tau} + \frac{(1-\alpha)r_0}{1 + \tau/\varphi_P}. \tag{G}$$

When the internal motion (φ_τ) of the protein is more rapid than the overall protein rotation (φ_P), then $\varphi_T \ll \varphi_P$, and the equation can be simplified as Eq. (H).

$$r(\tau) = \frac{\alpha r_0}{1 + \tau/\varphi_\tau} + \frac{(1-\alpha)r_0}{1 + \tau/\varphi_P} \tag{H}$$

Relative importance of each motion can be determined by the amplitude α and by the ratio of τ/φ_T and τ/φ_P. If $\alpha = 0$, the residue is immobile relative to the macromolecule, and the anisotropy is determined by the value of φ_P. If the residue is completely free to rotate, independent of the protein molecular motion, then $\alpha = 1$, and the anisotropy would be determined by φ_T. Now suppose the α is nonzero but less than one, and the overall rotational time is much larger than the fluorescence life time $\varphi_P \gg \tau$, then the rotation of the entire protein does not result in any loss of anisotropy, and the values for $r(\tau)$ are determined by the time scale of the internal motion (φ_T) and by the amplitude of this motion (α). If an internal motion is more rapid than the shortest quenched lifetime, $\varphi_T \ll \tau$, the effect of internal motion is complete prior to emission, and the overall rotation of the protein determines the decay of the residual anisotropy, $r_0(1 - \alpha)$. The existence of internal motion would be judged from the value of the anisotropy at $\tau = 0$.

In general, one can relate the anisotropy to the angular displacement (θ), also known as semicone angle, of the fluorophore according to

$$\theta = \cos^{-1}\left\{1/2\left[\left(1 + 8(r_\alpha/r_0)^{1/2}\right)^{1/2} - 1\right]\right\}. \tag{I}$$

A value of 0° corresponds to no rotational freedom, and an angle of 54.7° corresponds to complete depolarization.

All the fluorescence anisotropy and lifetime measurements were made with ISS K2 fluorimeter, using 300 nm LED as a light source. In our fitting model we considered only two components of fluorescence lifetime and rotational correlation time. Also faster component of anisotropy (r_1) was kept fixed to have acceptable deviation. Fitting of the experimental data was performed in Vinci software. For finding the right model, the following criteria were established to reject an analysis as unacceptable [17]:

1) If the normal standard of good fit (χ^2, residuals) were not satisfactory (χ^2 close to 1 with least residuals)
2) If any term r_i is ≤ 0 or ≥ 0.4;
3) If $r_i + r_j$ is ≥ 0.4;
4) If φ_1 and φ_2 is within 25% of each other;
5) If $\varphi_1 > \varphi_2$.
6) χ^2 curve.

3. Results

3.1. Resolution of rotational correlation time of BoNT/A LC

To obtain information about internal flexibility in BoNT/A LC we used a sensitive method of monitoring the frequency domain fluorescence anisotropy decay. This method resolves macromolecular tumbling from its local motion, and works well both with intrinsic as well as extrinsic probes [18–20]. In this work we used Trp as an intrinsic probe. BoNT/A LC is known to have two Trp residues, W43 and W118. An excitation wavelength of 300 nm was chosen, as Trp residues in protein can be selectively excited at this wavelength without exciting Tyr residues [21]. Also, excitation at 300 nm allows a high initial anisotropy due to lower emission intensity. This gives advantage in measurements by having high limiting anisotropy. The emission anisotropy decay was measured under six different conditions: set A) BoNT/A LC at 10 °C and 25 °C, set B) BoNT/A LC in 20% glycerol at 10 °C and 25 °C, and set C) BoNT/A LC in 50% glycerol at 10 °C and 25 °C. For each set of experiments triplicate measurements were carried out separately. Phase and modulation anisotropy decay curves recorded for BoNT/A LC at 10 °C and 25 °C are shown in Fig. 1 and 2, respectively. The raw data were fitted with the help of Vinci software provided by ISS (Urbana-Champaign, IL). Data were fitted with one, two, and three components. Final data values were determined according to criteria explained in the Materials and method section. One component analysis resulted in a wrong value of anisotropy showing large deviation, and three components resulted in large deviation in the third component of rotational time. Thus two component fittings were considered as the best fit for our rotational correlation time data.

Two distinct rotational correlation times were observed for BoNT/A LC, suggesting the existence of two kinds of rotational motions in this protein (Table 1). For the sake of simplicity in calculation, value of r_1 was fixed in most of the analysis. Before fixing, value of r_1 was optimized based on χ^2, residuals and deviation of floating parameters. Whereas at 25 °C, the Trp residue in BoNT/A LC exhibited both local segmental motion ($\varphi_1 \sim 0.15$ ns and $r_1 = 0.15$) and global slow rotational motion ($\varphi_2 \sim 9.2$ ns and $r_2 = 0.18$) indicating a degree of flexibility in the Trp containing peptide. However, at 10 °C the Trp residue in this protein exhibited only single and relatively slow rotational correlation time ($\varphi_2 \sim 9.1$ ns and $r_1 = 0.19$; Table 1), corresponding to only global motion of the protein. Raw data, curve fit data and residuals are shown in supplementary material (Fig. SM1 and SM2).

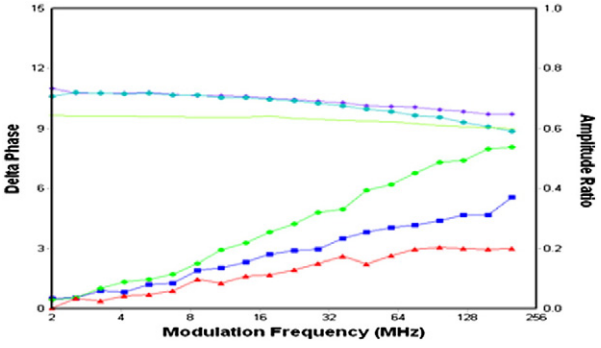

Fig. 1. BoNT/A LC anisotropy decay data without glycerol (▲ (phase), — (modulation)), with 20% glycerol (■ (phase), ◆ (modulation)) and with 50% glycerol (● (phase), ● (modulation)) at 10 °C. Protein was dissolved in 10 mM sodium phosphate buffer, pH = 7.3, containing 150 mM NaCl and 1 mM DTT.

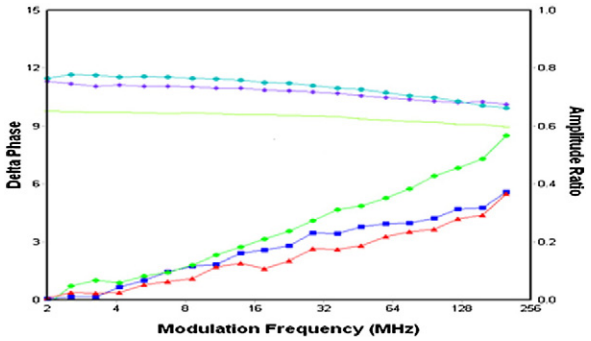

Fig. 2. BoNT/A LC anisotropy decay data without glycerol (▲ (phase), — (modulation)), with 20% glycerol (■ (phase), ◆ (modulation)) and with 50% glycerol (● (phase), ● (modulation)) at 25 °C. Protein was dissolved in 10 mM sodium phosphate buffer, pH = 7.3, containing 150 mM NaCl and 1 mM DTT.

3.2. Effect of viscosity on the rotational correlation time

Anisotropy decay data were collected in three different conditions (0, 20 and 50% glycerol) at two different temperatures (10 and 25 °C). Comparing the rotational correlation times of BoNT/A LC dissolved in buffer with no glycerol (described above) and with 20% and 50% glycerol at 10 °C, it was observed that the local segmental motion, which was undetected in buffer, gets slowed down to ~0.22 ns in 20% glycerol and finally ~0.50 ns in 50% glycerol (Table 1). The global component also became slower in 50% glycerol (φ_2 from ~9.1 to ~12.70 ns). These observations were expected as increased viscosity is expected to slow down the molecular or even segmental motions. However, at 10 °C the global

Table 1
Rotational correlation time data by frequency domain anisotropy decay analysis of BoNT/A LC in different conditions.

Sample	Rotational correlation times		Anisotropy		Lifetime	χ^2
	φ_1 (ns)	φ_2 (ns)	r_1	r_2	τ (ns) (F)	
LCA at 10 °C 0% glycerol-I	NA	9.11	NA	0.19	2.38	0.98
LCA at 10 °C 0% glycerol-II	NA	9.13	NA	0.19	2.37	0.89
LCA at 10 °C 0% glycerol-III	NA	8.88	NA	0.19	2.35	1.06
LCA at 25 °C 0% glycerol-I	0.13	9.2	0.15 (F)	0.18	2.13	1.17
LCA at 25 °C 0% glycerol-II	0.15	9.04	0.15 (F)	0.18	2.13	1.34
LCA at 25 °C 0% glycerol-III	0.17	9.3	0.15 (F)	0.18	2.1	1.13
LCA at 10 °C 20% glycerol-I	0.2	16.1	0.17 (F)	0.12	6.01	0.44
LCA at 10 °C 20% glycerol-II	0.21	18.2	0.18 (F)	0.13	6	0.44
LCA at 10 °C 20% glycerol-III	0.24	23.3	0.18 (F)	0.13	6.6	0.39
LCA at 25 °C 20% glycerol-I	0.21	23.2	0.17 (F)	0.11	7.35	0.65
LCA at 25 °C 20% glycerol-II	0.21	21	0.16 (F)	0.11	6.95	0.63
LCA at 25 °C 20% glycerol-III	0.18	20.8	0.16 (F)	0.13	6.35	0.57
LCA at 10 °C 50% glycerol-I	0.49	13.1	0.15 (F)	0.15	5.76	1.41
LCA at 10 °C 50% glycerol-II	0.48	13.8	0.15 (F)	0.15	5.79	0.71
LCA at 10 °C 50% glycerol-III	0.56	11.2	0.15 (F)	0.13	5.95	0.65
LCA at 25 °C 50% glycerol-I	0.19	7.53	0.20 (F)	0.13	4.24	1.46
LCA at 25 °C 50% glycerol-II	0.22	10.7	0.20 (F)	0.13	4.71	0.65
LCA at 25 °C 50% glycerol-III	0.23	7.41	0.17 (F)	0.12	4.27	1.21

component of the protein rotated slower (φ_2 ~ 22 ns) when dissolved in 20% glycerol compared to the protein solution with 50% glycerol (φ_2 ~ 13 ns). Also, r_1 changed in 20% glycerol (0.18 vs. 0.15) compared with no glycerol, whereas it was similar in 50% glycerol ($r_1 = 0.15$) (Table 1).

At 25 °C, emission anisotropy decay data showed a different trend with detectable segmental motion of 0.15 ns for the fast component, which increased to 0.20 ns in 20% glycerol and in 50% glycerol. However, the slow global component showed similar trend as that at 10 °C. The φ_2 was ~9.1 ns in buffer, which increases to ~21 ns in 20% glycerol (Table 1). Surprisingly, φ_2 decreased to ~9 ns in 50% glycerol. At this temperature r_1 increases with values of 0.15 in no glycerol, 0.16 in 20% glycerol and 0.19 in 50% glycerol, whereas r_2 decreases with values of 0.18 in no glycerol, 0.12 in 20% glycerol and 0.13 in 50% glycerol (Table 1). Raw data, curve fit data, and residuals are shown in supplementary materials (Fig. SM1 to SM6). For fitting of the data for the lifetime and rotational correlation times delta phase was 0.35 and amplitude ratio was 0.005.

The amplitude of the rotational motion can be interpreted as rotation angle of the fluorophore, as described in Eq. (A). Trp residue in BoNT/A LC in buffer at 10 °C appears to have no rotation freedom or undetected rotational movement. This is because of undetectable local motion. Although at 25 °C, tryptophan in local micro-environment had semicone angle less than that of whole molecule (semicone angle was 40.55° compared to 35.90°). With increasing glycerol, as expected global movement slows down but surprisingly tryptophan in local microenvironment was moving rapidly with semicone angle of ~34° in 20% glycerol (Table 3).

We examined the χ^2 surface to evaluate the significance and independence of the values listed in Table 1. χ^2 Surface of correlation times of BoNT/A LC is shown in their respective conditions (Supplementary materials, Fig. SM1 to SM6). Specifically, we held one correlation time fixed and floated other floating parameters. X-axis is the value of fixed correlation times and y-axis is the value of observed χ^2 value. χ^2 surface showed that the values are significant and independent from other components.

3.3. Effect of viscosity on the structure and function of BoNT/A LC

Rotational correlation time analysis by fluorescence anisotropy decay provides information about segmental and global motions. In general, global motion is affected by viscosity while the effect of viscosity on the local motion depends on the structural features of macromolecule. Notably, rotational correlation time data (described above) of BoNT/A LC showed the effect of viscosity on both the local and global motions (Table 1). Effect on local motion by viscosity indicated structural changes in the molecule, resulting in differential accessibility of glycerol to the protein matrix. Interestingly global motion of BoNT/A LC in 20% glycerol slowed down (~20 ns) more than in 50% glycerol (~10 ns). In order to explain this unexpected observation we examined the change in secondary and tertiary structures of BoNT/A LC in the presence of glycerol.

Far UV/CD spectral recordings and thermal denaturation, monitored by following CD signals at 222 nm, were employed to examine secondary structural changes in BoNT/A LC by glycerol. With increasing glycerol concentration, ellipticity at 222 nm for BoNT/A LC increased from about −25 mdeg to −35 mdeg as the concentration of glycerol was increased to 50% (Fig. 3). Increase in ellipticity at 222 nm is indicative of increase in α-helicity of the molecule (Fig. 3). To evaluate the thermal stability of different conformation of BoNT/A LC we measured the change in ellipticity at 222 nm at different temperatures. Thermal denaturation curves (Fig. 4) indicated that increased glycerol concentration resulted in higher Tm values (Table 2), Sharpness of the sigmoidal shape of the denaturation curve can provide information on the cooperativity of a protein unfolding. The denaturation curve for BoNT/A LC dissolved in 20% glycerol showed the sharpest denaturation curve, with a denaturation temperature span of 220 K–233 K. The melting temperature of BoNT/A LC, however, showed steady increase (~320 K to ~334 K) with the increase in the glycerol concentration from 0% to 50%. Increased Tm indicated that the stability of protein increased upon increase in glycerol concentration. Analysis of the denaturation curves to derive thermodynamic parameters provided measure of change in enthalpy (ΔH) and entropy (ΔS) of the protein unfolding (Table 2). ΔH of thermal denaturation first decreased from 477.9 ± 7.7 kJ/mol in a buffer with no glycerol to 395.8 ± 0.2 kJ/mol in buffer containing 20% glycerol, but showed steady increase beyond 20% glycerol, ultimately reaching a value of 427.6 ± 20.1 kJ/mol in a buffer containing 50% glycerol (Table 2). Notably, ΔS becomes less positive from 1424.5 ± 0.0 J/mol/K in a buffer with no glycerol to 1213 ± 2.1 J/mol/K in a buffer containing 20% glycerol, but also showed a steady increase in higher glycerol concentrations, reaching a value of 1362.4 ± 0.0 J/mol/K in a buffer containing 50% glycerol.

We also examined the thermal denaturation of tertiary structure by taking the ratio of fluorescence intensity at 351 nm and 324 nm. Trp emission maxima of 324 nm was observed for the native folded BoNT/A LC when excited at 295 nm, the emission maxima 351 nm was observed for free Trp, which can be assumed to be the emission maxima of Trp in the unfolded protein. Plotting the ratio of fluorescence intensity at 351 nm and 324 nm as a function of temperature showed a sigmoidal shape curve (Fig. 5), which allowed the estimation of inflection point as the melting temperature of the tertiary structure (Table 4).

Table 3
Semicone angles of local and global rotation.

Sample	Semicone angle	
	θ_1 (deg)	θ_2 (deg)
LCA at 10 °C 0% glycerol	NA	0.00
LCA at 25 °C 0% glycerol	40.55 ± 0.00	35.90 ± 0.00
LCA at 10 °C 20% glycerol	33.73 ± 0.30	42.27 ± 0.00
LCA at 25 °C 20% glycerol	33.54 ± 1.18	41.97 ± 1.30
LCA at 10 °C 50% glycerol	37.81 ± 0.00	38.42 ± 1.06
LCA at 25 °C 50% glycerol	33.21 ± 0.60	42.83 ± 0.48

Table 2
Thermodynamic parameters of secondary structure thermal denaturation of BoNT/A LC in different % of glycerol.

% Glycerol	ΔH (kJ/mol)	ΔS (J/(mol * K))	T_m (K)
0	477.90 ± 7.70	1424.50 ± 0.00	320.50 ± 0.00
10	409.80 ± 20.90	1266.70 ± 68.10	323.20 ± 0.90
20	395.80 ± 0.20	1213.00 ± 2.09	326.50 ± 0.00
40	428.20 ± 8.80	1291.80 ± 27.70	331.30 ± 0.20
50	427.60 ± 20.10	1362.40 ± 0.00	334.00 ± 0.40

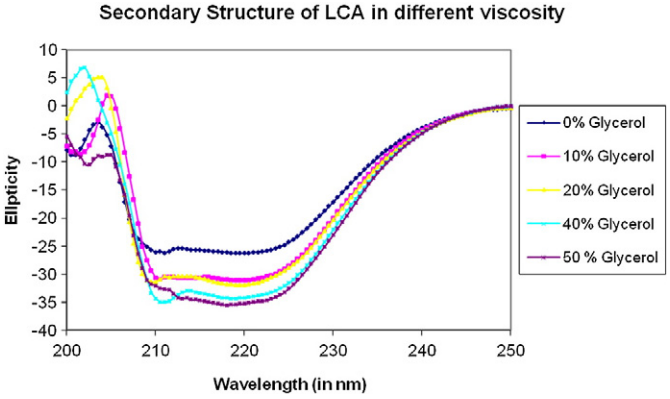

Fig. 3. Secondary structure of BoNT/A LC monitored by far UV-CD in 10 mM sodium phosphate buffer, pH = 7.3, containing 150 mM NaCl and 1 mM DTT. Percentage of glycerol in buffer is shown in the box.

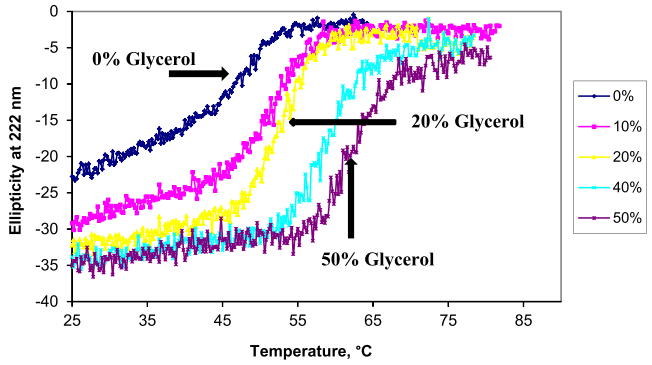

Fig. 4. BoNT/A LC thermal denaturation of secondary structure by measuring ellipticity at 222 nm with respect to temperature. BoNT/A LC was dissolved in 10 mM sodium phosphate buffer, pH = 7.3, containing 150 mM NaCl and 1 mM DTT. Thermal denaturation was measure for BoNT/A light chain without glycerol and with 10%, 20%, 40%, and 50% glycerol.

BoNT/A LC tertiary structure denaturation showed a trend different from the thermal denaturation of the secondary structure in terms of steady changes in denaturation patterns, although trend of the melting temperature of both the secondary (320.5 K–334.0 K) and tertiary structure (320.5 K–333.5 K) was the same. ΔH of thermal denaturation decreased from 453.5 ± 1.9 kJ/mol in a buffer with no glycerol to 271.0 ± 13.1 kJ/mol in buffer containing 50% glycerol (Table 4). Also ΔS becomes less positive from 1410.9 ± 31.5 J/mol/K in a buffer with no glycerol to 813.2 ± 59.4 J/mol/K in a buffer containing 50% glycerol. Difference in thermodynamic parameters obtained for tertiary structure and secondary structure indicates differential folding of secondary and tertiary structure, especially in the presence of glycerol.

Both secondary and tertiary structures were substantially stabilized by the presence of glycerol (Tm increase of 14 °C; Tables 2 and 4). While there is no uniformity in stability response of protein to glycerol [22,23], at least some level of stability is expected from the decreased molecular motion in glycerol due to increased viscosity. However, it was unusual to observe substantial change in the secondary structure, which is not commonly observed with other proteins [24,25], including thermolysin (data not shown), a metalloprotease with identical active site as BoNT endopeptidases.

In order to examine the effect of structural change introduced by glycerol on the function of BoNT/A LC, we assayed its endopeptidase activity using full length substrate His-tag SNAG. BoNT/A LC was enzymatically fully active in 10% glycerol, but the activity continued to decrease with further increase in glycerol concentration in the reaction buffer. The activity was decreased by 11, 21, and 24% in 20, 40, and 50% glycerol, respectively (Supplementary Fig. SM7).

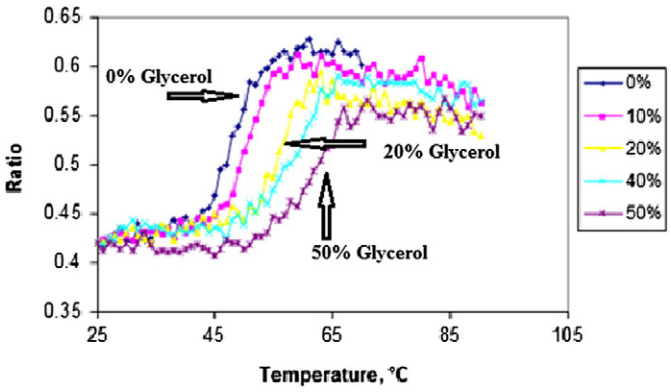

Fig. 5. Ratio of fluorescence intensity at 351 and 324 nm was plotted against the temperature to get the thermal denaturation profile of tertiary structure of BoNT/A LC. Tertiary structure thermal denaturation was measured for BoNT/A LC without glycerol and with 10%, 20%, 40% and 50% glycerol.

Table 4
Thermodynamic parameters of tertiary structure thermal denaturation of BoNT/A LC in different % of glycerol.

% Glycerol	ΔH (kJ/mol)	ΔS (J/(mol * K))	T_m (K)
0	453.50 ± 1.90	1410.90 ± 31.50	320.50 ± 0.00
10	406.20 ± 18.40	1256.70 ± 42.80	323.50 ± 0.00
20	374.20 ± 15.50	1141.60 ± 75.50	328.00 ± 1.10
40	281.60 ± 11.20	849.15 ± 30.50	332.50 ± 0.00
50	271.00 ± 13.10	813.23 ± 59.40	333.5 ± 0.00

4. Discussion

Molecular motions play a dramatic role in the recognition of unique whole protein substrates of BoNT endopeptidases, as has been concluded from X-ray structures of the co-crystals of BoNT/A and its substrate, SNAP-25 [13]. This conclusion was primarily based on the fact that crystal structures of all the confirmed seven serotypes of BoNT LCs remain essentially the same, and major segments which vary in their topography of different BoNT LCs are the loop regions [26]. It should be noted, however, that the interactions of the whole substrate with the endopeptidase occur at multiple sites, including α- and β-exosites, in addition to the active site. It is quite conceivable that these multiple sites exhibit conformational flexibility to accommodate a 206 amino acid reside substrate. Our interest has been to address a question of the molecular motions beyond the surface regions involved in the substrate recognition and binding.

The intrinsic protein fluorescence provides important information about the internal dynamics of a protein, which ultimately defines the structural and functional features of the protein. Fluorescence emission decay of intrinsic fluorophores like Trp is dependent on the conformations as well as interconversion rates among substates. One of the parameters of protein motion is defined as rotational correlation time (τc or ϕ), which measures tumbling of a molecule that in turn depends on size, shape and dynamics of the molecule as well as on the bulk physical characteristic of the solvent. Rotational correlation time can be obtained from the fluorescence decay and related to rotational diffusion coefficient; D_r. It is related to molecular volume V and depends on the solvent viscosity η [27–30]. By resolving the components of rotational correlation time we have been able to differentiate the global, local or segmental motion in BoNT/A LC to understand internal molecular motions.

The two components of rotational correlation time (RCT) with values of 0.15 ns and 9.2 ns at 25 °C suggest that the fast component reflects a local or segmental motion of the peptide segment containing the fluorescent Trp residue. Assuming only one of the two Trp residues is fluorescent, the fast component of the RCT would correspond to a segment containing one of the two Trp residues. To distinguish further the two types of motions (segmental and molecular), we carried out RCT determination in different concentrations of glycerol. Paradoxically, both the slow and fast RCT corresponding to the segmental and molecular motions changed with the increase in viscosity due the presence of glycerol (Table 1), which can be due to a) conformational changes introduced by the glycerol, b) penetration of glycerol to the interior of the protein, or c) both. These observations can be explained by assuming one of the following conditions: (i) The protein becomes more compact in the interior part of the molecule, and thus lowering the rotation radius, and (ii) The BoNT/A LC molecular shape does not remain globular, and perhaps assumes a distorted elliptical shape, again effectively reducing the rotational radius allowing protein interior to be more accessible. CD and fluorescence structural studies of BoNT/A LC in different glycerol concentrations reveal substantial changes in conformation of this molecule (Fig. 3–5), including a clear indication of more rigid structure in 50% glycerol. Although, BoNT/A LC appears to be rigid in 50% glycerol its global motion (φ_2 ~ 9 ns at 25°), in particular, is faster than the protein in 20% glycerol (φ_2 ~ 22 ns at 25°) indicating a more flexible structure. These observations suggest that increase in glycerol might

result in conformational changes which allow this molecule to move faster at 25 °C (Tables 1 and 2). Generally, glycerol is known to affect the stability of the protein [23, 30], but structural changes due to viscosity have not been reported.

Since glycerol was able to change the secondary and tertiary structures of BoNT/A LC, these structural changes indicate internal flexibility of BoNT/A LC. The flexibility of BoNT/A LC has been proposed previously based on X-ray crystallography and spectroscopic analysis of this protein under various temperature, pH, and chemical conditions [7,9,31, 32]. The behavior of the short and long components of the rotational correlation times with change in temperature and viscosity suggests that internal flexibility exists in BoNT/A LC. For example, non-observation of the short correlation time at 10 °C, which appears in 20% glycerol (Table 1) establishes the fact that glycerol is able to penetrate the protein matrix, alter the protein folding, leading to the resolution of the segmental motion from the molecular motion. This observation is supported by the resolution of the short rotational correlation time at higher temperature, which will obviously introduce faster segmental motion. The higher temperature, however, did not show faster molecular motion, perhaps owing to decrease in the compactness of the protein. Addition of 20% glycerol decreases the molecular motion, as would be expected with increase in viscosity of the solution. However, with 50% glycerol we observed unexpectedly increased molecular motion both at 10 and 25 °C, which could be explained only by the structural changes introduced by glycerol as was revealed by change in CD signals (Fig. 3). Interestingly the short rotational correlation time increased at 10 °C in 50% glycerol but remained the same at 25 °C, indicating a balancing effect of the temperature on the segmental motion even in the presence of higher amount of glycerol. In summary, the results indicate that the inner domains of the BoNT/A LC protein matrix are accessible to small molecules and that its segmental motions are liable to change in viscosity and temperature, suggesting significant flexibility of its conformation. These observations also complement our earlier findings in urea denaturation. The denaturation of BoNT/A LC by urea was shown to have a unique pattern [33], which was also explained to be due to its flexible structure.

In conclusion, the present study demonstrates that BoNT/A endopeptidase is holistically a flexible protein structure, readily modulated by environmental conditions like temperature and viscosity. Internal segmental motion and overall global tumbling was substantially affected by viscosity, suggesting the protein segments to be quite accessible due to its flexible structure. In addition to changes in size and shape which may be involved in BoNT/A endopeptidase interaction with its substrate, molecular dynamics should also be examined to learn about this very unique enzyme–substrate system currently available. Such information will be helpful in designing small molecule inhibitors against BoNT endopeptidases.

Appendix A. Supplementary data

Supplementary data to this article can be found online at http://dx.doi.org/10.1016/j.bbapap.2014.12.004.

References

[1] M. Hallett, One man's poison: clinical applications of botulinum toxin, N. Engl. J. Med. 341 (1999) 118–129.
[2] F.J. Erbguth, From poison to remedy: the chequered history of botulinum toxin, J. Neural Transm. 115 (4) (2008) 559–565.
[3] J. Jankovic, Botulinum toxin in clinical practice, J. Neurol. Neurosurg. Psychiatry 75 (2004) 951–957.
[4] F.N. Fu, R.B. Lomneth, S. Cai, B.R. Singh, Role of zinc in the structure and toxic activity of botulinum neurotoxin, Biochemistry 37 (1998) 5267–5278.
[5] S. Cai, B.R. Singh, Role of disulfide-cleavage induced molten globule state of type A botulinum neurotoxin in its endopeptidase activity, Biochemistry 40 (2001) 15327–15333.
[6] L. Li, B.R. Singh, Role of zinc binding in type A botulinum neurotoxin light chain's toxic structure, Biochemistry 39 (2000) 10581–10586.
[7] R.V. Kukreja, B.R. Singh, Biologically active novel conformational state of botulinum, the most poisonous poison, J. Biol. Chem. 280 (2005) 39346–39352.
[8] P. Washbourne, R. Pellizzari, G. Baldini, M.C. Wilson, C. Montecucco, Botulinum neurotoxin types A and E require the SNARE motif in SNAP-25 for proteolysis, FEBS Lett. 418 (2000) 1–5.
[9] N.R. Silvaggi, G.E. Boldt, M.S. Hixon, J.P. Kennedy, S. Tzipori, K.D. Janda, K.N. Allen, Structures of *Clostridium botulinum* neurotoxin serotype A light chain complexed with small-molecule inhibitors highlight active-site flexibility, Chem. Biol. 14 (2007) 533–542.
[10] S. Easwaramoorthy, D. Kumaran, S. Swaminathan, A novel mechanism for *Clostridium botulinum* neurotoxin inhibition, Biochemistry 41 (2002) 9795–9802.
[11] R. Agarwal, S. Eswaramoorthy, D. Kumaran, T. Binz, S. Swaminathan, Structural analysis of botulinum neurotoxin type E catalytic domain and its mutant Glu212 → Gln reveals the pivotal role of the Glu212 carboxylate in the catalytic pathway, Biochemistry 43 (2004) 6637–6644.
[12] B. Segelke, M. Knapp, S. Kadkhodayan, R. Balhorn, B. Rupp, Crystal structure of *Clostridium botulinum* neurotoxin protease in a product-bound state: evidence for non-canonical zinc protease activity, PNAS 101 (2004) 6888–6893.
[13] M.A. Breidenbach, A.T. Brunger, Substrate recognition strategy for botulinum neurotoxin serotype A, Nature 432 (2004) 925–929.
[14] R.V. Kukreja, S.K. Sharma, B.R. Singh, Molecular basis of activation of endopeptidase activity of botulinum neurotoxin type E, Biochemistry 49 (2010) 2510–2519.
[15] L.M. Eubanks, P. Silhar, N.T. Salzameda, J.S. Zakhari, F. Xiaochuan, J.T. Barberi, C.B. Shoemaker, M.S. Hixon, K.D. Janda, Identification of a natural product antagonist against the botulinum neurotoxin light chain protease, ACS Med. Chem. Lett. (2010) 268–272.
[16] T.W. Chang, Sequence Analyses and Novel Antidotes Development of Botulinum Neurotoxin(Thesis dissertation) UMASS Dartmouth, 2011. (143).
[17] C.N. Bialik, B. Wolf, E.L. Rachofsky, J.B.A. Ross, W.R. Laws, Fluorescence anisotropy decay: finding the correct physical model, Proc. SPIE Int. Soc. Opt. Eng. 3256 (1996) 60–67.
[18] J.R. Lackowicz, Principle of Fluorescence Spectroscopy, Plenum Press, New York, 1983. 111–114.
[19] K. Takeda, I. Yoshida, K. Yamamoto, Changes of fluorescence lifetime and rotational correlation time of bovine serum albumin labeled with 1-dimethylaminonaphthalene-5-sulfonyl chloride is guanidine and thermal denaturation, J. Protein Chem. 10 (1) (1991) 17–63.
[20] O. Tcherkasskaya, O.B. Ptitsyn, J.R. Knutson, Nanosecond dynamics of tryptophans in different conformal states of apomyoglobin proteins, Biochemistry 39 (2000) 1879–1889.
[21] J.R. Lakowicz, B.P. Maliwal, H. Cherek, A. Balter, Rotational freedom of tryptophan residues in proteins and peptides, Biochemistry 22 (8) (1983) 1741–1752.
[22] K. Gekkof, S.N. Timasheff, Thermodynamic and kinetic examination of protein stabilization by glycerol, Biochemistry 20 (1981) 4677–4686.
[23] T. Knubovets, J.J. Osterhout, P.J. Connolly, A.M. Klibanov, Structure, thermostability, and conformational flexibility of hen egg-white lysozyme dissolved in glycerol, PNAS 96 (1999) 1262–1267.
[24] G.S. Lakshmikanth, G. Krisnamoorthy, Solvent-exposed tryptophans probe the dynamics at protein surfaces, Biophys. J. 77 (1999) 1100–1106.
[25] C. Bongiovanni, F. Sinibaldi, T. Ferri, R. Santucci, Glycerol-induced formation of the molten globule from acid-denatured cytochrome c: implication for hierarchical folding, J. Protein Chem. 21 (2002) 35–41.
[26] A.T. Brunger, A. Rummel, Receptor and substrate interactions of clostridial neurotoxins, Toxicon 54 (2009) 550–560.
[27] J.R. Lakowicz, G. Laczko, I. Gryczynski, H. Cherek, Measurement of subnanosecond anisotropy decays of protein fluorescence using frequency-domain fluorometry, J. Biol. Chem. 261 (1983) 2240–2245.
[28] E. Bismuto, E. Gratton, I. Sirabgelo, G. Irace, Structure and dynamics of the acidic compact state of apomyoglobin by frequency-domain fluorometry, Eur. J. Biochem. 218 (1993) 213–219.
[29] J.B.A. Ross, K.W. Roussiang, L. Brand, Time resolved fluorescence and anisotropy decay of the tryptophan in adrenocorticotropin-(1–24), Biochemistry 20 (1981) 4361–4369.
[30] T. Ichiye, M. Karplus, Fluorescence depolarization of Trp residues in proteins: a molecular dynamics study, Biochemistry 22 (1983) 2884–2893.
[31] S. Cai, R. Kukreja, S. Shoesmith, T.W. Chang, B.R. Singh, Botulinum neurotoxin light chain refolds at endosomal pH for its translocation, Protein J. 25 (2007) 455–462.
[32] J.C. Burnett, B. Li, R. Pai, S.C. Cardinale, S.C. Butler, M.M. Butler, N.P. Peet, D. Moir, S. Bavari, T. Bowlin, Analysis of botulinum neurotoxin serotype A metalloprotease inhibitors: analogs of a chemotype for therapeutic development in the context of a three-zone pharmacophore, Open Access Bioinformatics 2 (2010) 11–18.
[33] R. Kumar, R. Kukreja, L. Li, A. Zhmurov, O. Kononova, S. Cai, S. Ahmed, V. Barsegov, B.R. Singh, Botulinum neurotoxin: unique folding of enzyme domain of the most poisonous poison, J. Biomol. Struct. Dyn. 32 (2013) 804–815.